Graphical Abstract

Isolation, structure determination and cytotoxicity studies of tryptophan alkaloids from an Australian marine sponge *Hyrtios* sp.

Leave this area blank for abstract info.

Shahan Khokhar, Yunjiang Feng, Marc R. Campitelli, Merrick G. Ekins, John N. A. Hooper, Karren D. Beattie, Martin C. Sadowski, Colleen C. Nelson, and Rohan A. Davis

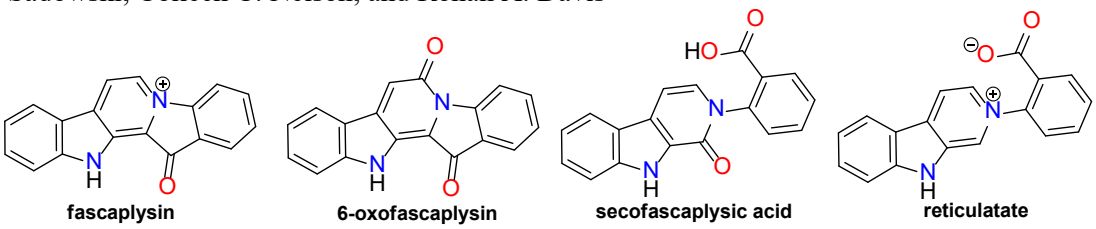

Isolation, structure determination and cytotoxicity studies of tryptophan alkaloids from an Australian marine sponge *Hyrtios* sp.

Shahan Khokhar[a], Yunjiang Feng[a], Marc R. Campitelli[a], Merrick G. Ekins[b], John N. A. Hooper[a,b], Karren D. Beattie[a], Martin C. Sadowski[c], Colleen C. Nelson[c], and Rohan A. Davis[a,*]

[a] *Eskitis Institute for Drug Discovery, Griffith University, Brisbane, QLD 4111, Australia.*
[b] *Queensland Museum, South Brisbane, QLD 4101, Australia*
[c] *Australian Prostate Cancer Research Centre – Queensland Institute of Health and Biomedical Innovation, Queensland University of Technology, Princess Alexandra Hospital, Translational Research Institute, Brisbane, QLD 4102, Australia.*

ARTICLE INFO

Article history:
Received
Revised
Accepted
Available online

Tryptophan alkaloid
Marine sponge
Hyrtios
DFT-NMR
Cytotoxicity

ABSTRACT

Mass-guided fractionation of the MeOH extract from a specimen of the Australian marine sponge *Hyrtios* sp. resulted in the isolation of two new tryptophan alkaloids, 6-oxofascaplysin (**2**), and secofascaplysic acid (**3**), in addition to the known metabolites fascaplysin (**1**) and reticulatate (**4**). The structures of all molecules were determined following NMR and MS data analysis. Structural ambiguities in **2** were addressed through comparison of experimental and DFT-generated theoretical NMR spectral values. Compounds **1**–**4** were evaluated for their cytotoxicity against a prostate cancer cell line (LNCaP) and were shown to display IC_{50} values ranging from 0.54 to 44.9 μM.

Marine sponges are a prolific source of structurally diverse and biologically active natural products, including alkaloids derived from tryptophan.[1] More than one quarter of marine alkaloids that have been isolated to date contain the indole skeleton, and in addition to their cytotoxic, antibacterial and antiviral activities, they often possess unusual structures and functional groups.[2] The sponge genus *Hyrtios* is a well-known source of these secondary metabolites, and a number of tryptophan alkaloids have been reported from Pacific specimens collected in Fiji, Indonesia and the Okinawan Islands.[3-7] Extracts of these specimens have yielded alkaloids related to fascaplysin (**1**),[8] such as homo-fascaplysin,[3] thorectandramine[5] and various brominated derivatives,[4] along with *β*-carboline alkaloids including hyrtioerectines,[9] hyrtioreticulins[10] and hyrtimomines D and E.[11] A number of these chemicals have demonstrated antimalarial, cytotoxic and antibacterial activities.[3,8,12,13] Owing to these reports of interesting tryptophan metabolites from *Hyrtios* specimens, we initiated a chemical investigation of several Australian samples available in the Eskitis Institute's Nature Bank biota repository,[14] with the ultimate goal of uncovering new tryptophan-derived alkaloids.

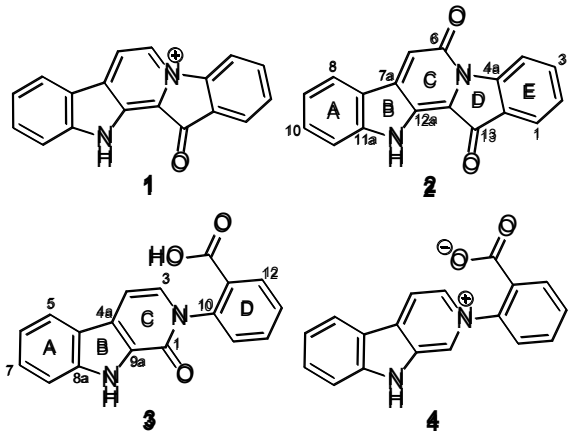

Figure 1. Structures of metabolites **1**–**4**

Several dried *Hyrtios* samples, which were available in large quantities (>100 g) from the Nature Bank biota repository, were initially chosen for chemical analysis. Small quantities of freeze-dried and ground sponge material were extracted with MeOH/H_2O (4:1), followed by LC-MS analysis.

* Corresponding author. Tel.: +61-7-3735-6043; fax: +61-7-3735-6001; e-mail: r.davis@griffith.edu.au

Table 1 NMR spectroscopic data for 6-oxofascaplysin (**2**)[a]

No.	^{13}C, exptl.	^{13}C, calcd.[b]	^{1}H (mult., *J* in Hz, int.)	HMBC	ROESY
1	123.6	124.1	7.81 (d, 7.6, 1H)	3, 4a, 13	2
2	126.0	124.5	7.38 (dd, 7.6, 7.6, 1H)	4, 13a	1, 3
3	135.6	135.6	7.74 (dd, 7.6, 8.0, 1H)	1, 4a	2, 4
4	117.4	116.3	8.62 (d, 8.0, 1H)	2, 4a, 13a	3
4a	146.1	146.2			
6	157.0	153.5			
7	119.4	119.7	7.51 (s, 1H)	6, 7a, 7b, 12a, 12b	8
7a	142.4	140.4			
7b	119.4	118.0			
8	123.8	124.3	8.07 (d, 7.7, 1H)	7a, 10, 11a	7, 9
9	121.1	119.9	7.15 (dd, 7.0, 7.7, 1H)	7b, 11	8, 10
10	132.1	132.6	7.52 (dd, 7.0, 7.0, 1H)	8, 11a	9, 11
11	112.1	110.1	7.37 (d, 7.0, 1H)	7b, 9	10
11a	147.4	144.0			
12-NH			11.65 (s, 1H)	7a, 7b, 11a, 12a	
12a	128.6	128.3			
12b	115.3	114.7			
13	180.2	177.5			
13a	124.4	121.8			
CMAD[c]		1.4			
MD[d]		3.5			

[a] Spectra were recorded in DMSO-d_6 (^{1}H at 600 MHz, ^{13}C at 150 MHz); [b] Theoretical data calculated in DMSO-d_6; [c] CMAD = corrected mean absolute deviation; [d] MD = maximum deviation.

One *Hyrtios* sponge extract[14] contained a strong ion at *m/z* 271, suggestive of the presence of fascaplysin (**1**), but also showed two pseudomolecular ions at *m/z* 287 and 305, which did not correspond to known *Hyrtios* metabolites following molecular weight (MW) searches using the Dictionary of Natural Products database (**Fig. 1**).[13] Thus, 10 grams of freeze-dried and ground sponge material was extracted and subjected to mass-guided fractionation. The compounds corresponding to the MS ions of interest (*m/z* 287 and 305) were purified using C_{18} HPLC (MeOH/H_2O/0.1% TFA), resulting in the isolation of the new molecules, 6-oxofascaplysin (**2**, 1.5 mg, 0.015% dry wt, MW 286) and secofascaplysic acid (**3**, 1.3 mg, 0.013% dry wt, MW 304). The previously reported alkaloids, fascaplysin (**1**, 26.0 mg, 0.260% dry wt) and reticulatate (**4**, 0.8 mg, 0.08% dry wt) were also isolated during these studies and were identified based on comparison of NMR and MS data with literature values (**Fig. 1**).[3,4] Compound **1** was originally reported from the Fijian sponge *Fascaplysinopsis* sp.,[8] whereas **4** is a known natural product from the Fijian sponge *F. reticulata*.[4]

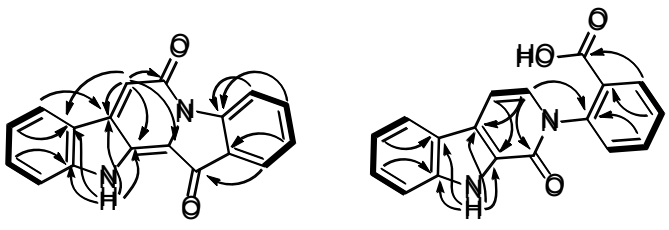

Figure 2. ^{1}H-^{1}H COSY (—) and selected HMBC (→) correlations for **2** and **3**

Compound **2**[15] was obtained as a dark red gum, with HRESIMS measurements confirming the molecular formula as $C_{18}H_{10}N_2O_2$ (15 degrees of unsaturation). The ^{1}H NMR spectrum displayed an exchangeable broad singlet (δ_H 11.65), four aromatic doublets (δ_H 7.37, 7.81, 8.07, 8.62), four aromatic doublets of doublets (δ_H 7.15, 7.38, 7.52, 7.74), and an additional isolated singlet (δ_H 7.51), which together accounted for all ten protons (**Table 1**). HSQC correlations enabled protons to be attached to their respective carbons. Eighteen carbons were observed from HSQC and HMBC spectroscopic data, including nine aromatic methine carbons and seven aromatic quaternary carbons. Two additional signals manifesting at δ_C 180.2 and 157.0 were attributed to a conjugated enone carbonyl and an amide carbonyl respectively. Analysis of the COSY spectrum of **2** showed two spins systems: δ_H 7.81, 7.38, 7.74 and 8.62; as well as δ_H 8.07, 7.15, 7.52 and 7.37 consistent with two 1,2-disubstituted benzene rings (rings E and A, **Figs. 1** and **2**). Ring E was found to be part of an indole system based on the HMBC couplings from H-3 (δ_H 7.74) and H-4 (δ_H 8.62) to C-4a (δ_C 146.1), and from H-1 (δ_H 7.81) to the conjugated enone C-13 (δ_C 180.2) in ring D (**Fig. 2**). Ring A was part of an additional indole unit, indicated by HMBC correlations from 12-NH (δ_H 11.65) to C-11a (δ_C 147.4) and C-7a (δ_C 142.4), C-7b (δ_C 119.4) and C-12a (δ_C 128.6). HMBC correlations from H-8 (δ_H 8.07) to C-7a and from 12-NH to C-7a and C-12a (δ_C 128.6) confirmed the pyrrolidine (ring B) of the indole subunit. The aromatic methine singlet, H-7 (δ_H 7.51) showed strong HMBC couplings to the amide carbonyl carbon resonating at δ_C 157.0 (C-6), as well as C-7a, C-7b and C-12a (**Fig. 2**). This indicated that H-7 was part of the conjugated enone, and linked directly to ring B through C-7a and ring D through the amide bond. A weak correlation was observed in the HMBC experiment ($^{n}J_{CH}$ = 3 Hz) from H-7 to C-12b (δ_C 115.3), indicating the formation of a lactam (ring C). However there were no NMR correlations to suggest that C-12b was connected to the ketone carbon through C-13; this was established based on the one remaining, and unaccounted for degree of unsaturation. The weakness of the observed C-12b signal, together with the ambiguity surrounding the connectivity between C-12b and C-13, presented us with an opportunity to use Density Functional Theory (DFT) NMR calculations to support our structure assignment. DFT is a branch of physics that has successfully been used in the past to justify or reassign molecular structures.[16-18] For these current studies, DFT calculations were initiated on compound **2**, with the molecule subjected to molecular mechanics energy minimization and subsequent conformational searches using MMFFs.[19] The minimum energy conformer was further optimized using DFT with the B3LYP/6-31G(d,p) functional and basis set combination.[20-22] Single-point calculations were performed using the MPW1PW91/6-311G(d,p) level of theory, incorporating implicit PBF solvation.[23,24] The output data was used to calculate NMR shielding constants via gauge including atomic orbitals (GIAO) methodology. Reference

Table 2 NMR spectroscopic data for secofascaplysic acid (**3**)[a]

No.	^{13}C, exptl.	^{13}C, calcd.[b]	^{1}H (mult., *J* in Hz, int.)	HMBC	ROESY
1	155.0	150.5			
3	128.7	129.1	7.29 (d, 7.0, 1H)	1, 4, 4a, 10	4
4	99.8	99.5	7.09 (d, 7.0, 1H)	9a	3, 5
4a	123.4	122.0			
4b	121.8	120.2			
5	121.0	121.1	8.07 (d, 8.0, 1H)	4a, 8a, 7	4, 6
6	119.4	118.2	7.20 (dd, 8.0, 8.0, 1H)	4b, 8	5, 7
7	126.2	126.2	7.42 (dd, 8.0, 8.4, 1H)	5, 8, 8a	6, 8
8	112.2	110.5	7.53 (d, 8.4, 1H)	4b, 6	9-NH
8a	139.2	135.8			
9-NH			12.02 (s, 1H)	4a, 4b, 8a, 9a	8
9a	127.4	124.7			
10	140.3	141.1			
11	129.9	125.8			
11-CO_2H	166.1	163.6	NO[e]		
12	130.1	129.8	7.99 (d, 8.1, 1H)	14, 11-CO_2H, 10	13
13	128.2	127.8	7.60 (dd, 8.1, 8.1, 1H)	11, 15	12, 14
14	132.8	134.2	7.75 (dd, 7.8, 8.1, 1H)	10, 12	15, 13
15	128.9	128.7	7.47 (d, 7.8, 1H)	11, 13	14
CMAD[c]		1.6			
MD[d]		4.5			

[a] Spectra were recorded in DMSO-d_6 (^{1}H at 600 MHz, ^{13}C at 150 MHz); [b] Theoretical data calculated in DMSO-d_6; [c] CMAD = corrected mean absolute deviation; [d] MD = maximum deviation; [e] NO = Not observed.

compounds with previously published experimental NMR data were used to generate a linear regression model, which correlated observed chemical shifts with the calculated shielding constants (see supplementary data S16). The multi-reference regression model was thus used to scale calculated shielding constants to give ^{13}C NMR shifts for **2**. The theoretical ^{13}C NMR data for **2** were compared to the experimental data (**Table 1**) and both sets of data were consistent with the chemical structure proposed. The greatest chemical shift deviation (Δ 3.5 ppm) between the theoretical and experimental data sets was attributed to the amide carbonyl carbon, C-6. Based on these theoretical calculations, the proposed structure of **2** was definitively assigned.

Compound **3**[25] was obtained as an orange-brown gum. The molecular formula was determined to be $C_{18}H_{12}N_2O_3$ on the basis of HRESIMS measurements and NMR data (14 degrees of unsaturation). Ten aromatic signals were noted in the ^{1}H NMR spectrum of **3**, as well as an additional exchangeable singlet at δ_H 12.02. The HSQC and HMBC spectra revealed the presence of ten methine aromatic carbons, seven quaternary aromatic carbon atoms, and two carbonyl carbon atoms resonating at δ_C 155.0 and 166.1 (**Table 2**). COSY correlations established three spin systems (**Fig. 2**). One system, part of ring A, consisted of a 1,2-disubstituted benzene rings as indicated by ^{1}H-^{1}H couplings between H-5 (δ_H 8.07), H-6 (δ_H 7.20), H-7 (δ_H 7.42) and H-8 (δ_H 7.53). Furthermore, an additional 1,2-disubstituted system (ring D) was deduced from COSY couplings between H-12 (δ_H 7.99), H-13 (δ_H 7.60), H-14 (δ_H 7.75) and H-15 (δ_H 7.47), and an isolated *cis* olefinic spin system was also observed (H-3, δ_H 7.29 and H-4 δ_H 7.09). Ring B was found to be part of an indole system, evident by the observation of HMBC couplings from H-6 (δ_H 7.20) to C-4b (δ_C 121.8) and H-7 (δ_H 7.42) to C-8a (δ_C 139.2). Further confirmation of the indole system of **3** was established on the basis of two- and three-bond HMBC correlations from the exchangeable NH (δ_H 12.02) to four quaternary carbons (C-4a, C-4b, C-8a, and C-9a), which constituted a pyrrolidine (ring B). In the HMBC, the olefinic protons H-3 (δ_H 7.29) and H-4 (δ_H 7.09) were found to couple to C-4a and C-9a respectively, situating the olefin adjacent to ring B (**Table 2**). A strong $^{3}J_{CH}$ HMBC correlation from H-3 was also observed to the amide carbon at δ_C 155.0 (C-1), and also δ_C 140.3 (C-10) of ring D. The characteristic chemical shift of C-10 indicated it was adjacent to a nitrogen atom, which linked ring D to the olefin through the nitrogen of the amide. The di-substituted benzene (ring D) was found to have a carbonyl functionality attached at C-11 (δ_C 129.9), owing to a HMBC correlation from H-12 to 11-CO_2H (δ_C 166.1). With all but an oxygen and hydrogen atom unaccounted for, the carbonyl functionality was designated as an acid. The remaining degree of unsaturation enabled a further ring closure through a bond between C-1 and C-9a, forming ring C and thus establishing the structure of compound **3**.

Since assigning functional groups and ring closures by remaining atoms and degrees of unsaturation always leaves an element of doubt as to a molecule's final structure, we decided to use the same principles of DFT used in **2** to validate the experimental NMR data of **3**. We also felt that applying DFT to the related structure, **3**, would consolidate its use as suitable for predicting NMR shifts for this particular class of alkaloid. Thus, compound **3** was subjected to molecular mechanics energy minimization and conformational searches using MMFFs. In this case, eight conformers were generated, which could be grouped into four pairs of similar conformers. The lowest energy conformer of each pair was then further optimized via DFT with the same functional and basis set as **2**. Single point calculations with the same conditions used to calculate **2** enabled NMR shielding constants to be generated, which were translated to theoretical NMR values using the linear regression model. The resulting data enabled the generation of theoretical chemical shifts for **3** (**Table 2**). These shifts were in good agreement with the experimental chemical shifts, with the greatest deviation evident for the amide carbonyl carbon (Δ 4.5 ppm, **Table 3**). These DFT data confirmed the proposed structure of **3**, and allowed us to conclude that DFT ^{13}C NMR analysis is a valid method for this particular structure class.

The cytotoxicity of fascaplysin and related alkaloids, such as reticulatate, has been well documented.[4,7] Biochemical studies have reported that fascaplysin is a DNA intercalator,[12] a potent and selective inhibitor of Cdk4, and it has also been shown to inhibit phosphorylation of the retinoblastoma protein Rb, resulting in G_0/G_1 phase cycle arrest of cancer cells.[26] Moreover, fascaplysin displays potent *in vitro* activity against numerous cancer lines, including MCF-7 (EC_{50} 0.14 μg/mL), MALME-3M

(EC_{50} 0.03 μg/mL) and OVCAR-3 (0.16 μg/mL).[5] Furthermore, brominated analogues of fascaplysin have shown activity against HL-60, THP-1, SNU-C4, SK-MEL-28, DLD-1, MDA-MB-231 and HeLa cancer cell lines.[27] The activity of these brominated alkaloids was determined to, in part, be the result of induction of caspase-8, -9 and -3 dependent apoptosis.[27] Additionally, reticulatate (**4**) has demonstrated activity against the murine C38 and human H116 cell lines.[4] Due to these previous reports of cytotoxic activity for this particular structure class, and our interest in identifying new prostate cancer small molecule inhibitors,[28] we decided to investigate the biological effects of **1**–**4** against an androgen-sensitive prostate cancer cell line, LNCaP, as well as non-malignant neonatal foreskin fibroblasts (NFF) in order to ascertain if these molecules displayed any selectivity towards LNCaP. With the Alamar Blue assay, it was demonstrated that all four compounds were cytotoxic towards LNCaP and NFF (**Table 3**). In particular, the most potent of the compounds, fascaplysin (**1**) displayed poor selectivity [LNCaP IC_{50} = 0.54 μM, NFF IC_{50} = 0.34 μM, selectivity index (SI) = 0.63], while the new derivative 6-oxofascaplysin (**2**) demonstrated a lower overall cytotoxicity (LNCaP IC_{50} = 22.90 μM, NFF IC_{50} = 32.11 μM) but slightly better selectivity (SI = 1.40).

Table 3 Cytotoxicity data for metabolites **1**–**4**

Compound	IC_{50} (μM)[a]		SI[d]
	LNCaP[b]	NFF[c]	
1	0.54	0.34	0.63
2	22.90	32.11	1.40
3	44.90	47.62	1.06
4	25.86	19.79	0.77
doxorubicin	0.01	0.13	8.97

[a] 50% inhibitory concentration; [b] LNCaP = human prostate cancer cell line; [c] NFF = human neonatal foreskin fibroblast cell line; [d] SI (selectivity index) = NFF IC_{50} / LNCaP IC_{50}

Acknowledgements

We thank G. MacFarlane from the University of Queensland for acquiring the HRESIMS measurements. We acknowledge R. Quinn from Griffith University for access to the four sponge samples that form part of the Nature Bank biota repository. SK would like to acknowledge the Australian Government for an Australian Postgraduate Award (APA) scholarship.

Supplementary data

Supplementary data [1D and 2D NMR spectra for 6-oxofascaplysin (**2**) and secofascaplysic acid (**3**), sponge taxonomic information, computational procedures and linear regression curves, extraction and purification conditions and cytotoxicity assay procedures] associated with this article can be found in the online version, at http://dx.doi.org/

References and notes

1. Blunt, J. W.; Copp, B. R.; Keyzers, R. A.; Munro, M. H. G.; Prinsep, M. R. *Nat. Prod. Rep.* **2013**, *30*, 237.
2. Gul, W.; Hamann, M. T. *Life Sci.* **2005**, *78*, 442.
3. Kirsch, G.; König, G. M.; Wright, A. D.; Kaminsky, R. *J. Nat. Prod.* **2000**, *63*, 825.
4. Segraves, N. L.; Lopez, S.; Johnson, T. A.; Said, S. A.; Fu, X.; Schmitz, F. J.; Pietraszkiewicz, H.; Valeriote, F. A.; Crews, P. *Tetrahedron Lett.* **2003**, *44*, 3471.
5. Charan, R. D.; McKee, T. C.; Gustafson, K. R.; Pannell, L. K.; Boyd, M. R. *Tetrahedron Lett.* **2002**, *43*, 5201.
6. Momose, R.; Tanaka, N.; Fromont, J.; Kobayashi, J. *Org. Lett.* **2013**, *15*, 2010.
7. Segraves, N. L.; Robinson, S. J.; Garcia, D.; Said, S. A.; Fu, X.; Schmitz, F. J.; Pietraszkiewicz, H.; Valeriote, F. A.; Crews, P. *J. Nat. Prod.* **2004**, *67*, 783.
8. Roll, D. M.; Ireland, C. M.; Lu, H. S. M.; Clardy, J. *J. Org. Chem.* **1988**, *53*, 3276.
9. Youssef, D.; Shaala, L.; Asfour, H. *Mar. Drugs* **2013**, *11*, 1061.
10. Yamanokuchi, R.; Imada, K.; Miyazaki, M.; Kato, H.; Watanabe, T.; Fujimuro, M.; Saeki, Y.; Yoshinaga, S.; Terasawa, H.; Iwasaki, N.; Rotinsulu, H.; Losung, F.; Mangindaan, R. E. P.; Namikoshi, M.; de Voogd, N. J.; Yokosawa, H.; Tsukamoto, S. *Bioorg. Med. Chem.* **2012**, *20*, 4437.
11. Tanaka, N.; Momose, R.; Takahashi, Y.; Kubota, T.; Takahashi-Nakaguchi, A.; Gonoi, T.; Fromont, J.; Kobayashi, J. *Tetrahedron Lett.* **2013**, *54*, 4038.
12. Hörmann, A.; Chaudhuri, B.; Fretz, H. *Bioorg. Med. Chem.* **2001**, *9*, 917.
13. Dictionary of Natural Products on DVD, version 21.2, ed., Chapman and Hall/CRC, Boca Raton, 2012.
14. For full information about the *Hyrtios* specimen see the supplementary data section
15. 6-Oxofascaplysin (**2**): red gum; UV (MeOH) λ_{max} (log ε) 225 (4.11), 275 (3.92), 314 (3.66), 535 (3.29) nm; ^{1}H and ^{13}C NMR data (DMSO-d_6), see Table 1; (+)-LRESIMS *m/z* 287 $[M + H]^+$; (+)-HRESIMS *m/z* 287.0817 $[M + H]^+$ (calcd for $C_{18}H_{11}N_2O_2$, 287.0815).
16. Smith, S. G.; Goodman, J. M. *J. Am. Chem. Soc.* **2010**, *132*, 12946.
17. Lodewyk, M. W.; Tantillo, D. J. *J. Nat. Prod.* **2011**, *74*, 1339.
18. Khokhar, S.; Feng, Y.; Campitelli, M. R.; Quinn, R. J.; Hooper, J. N. A.; Ekins, M. G.; Davis, R. A. *J. Nat. Prod.* **2013**, *76*, 2100.
19. Halgren, T. A. *J. Comput. Chem.* **1999**, *20*, 720.
20. Becke, A. D. *J. Chem. Phys.* **1993**, *98*, 5648.
21. Lee, C.; Yang, W.; Parr, R. G. *Phys. Rev. B.* **1988**, *37*, 785.
22. Vosko, S. H.; Wilk, L.; Nusair, M. *Can. J. Phys.* **1980**, *58*, 1200.
23. Tannor, D. J.; Marten, B.; Murphy, R.; Friesner, R. A.; Sitkoff, D.; Nicholls, A.; Honig, B.; Ringnalda, M.; Goddard, W. A. *J. Am. Chem. Soc.* **1994**, *116*, 11875.
24. Marten, B.; Kim, K.; Cortis, C.; Friesner, R. A.; Murphy, R. B.; Ringnalda, M. N.; Sitkoff, D.; Honig, B. *J. Phys. Chem.* **1996**, *100*, 11775.
25. Secofascaplysic acid (**3**): brown/orange gum; UV (MeOH) λ_{max} (log ε) 243 (4.40), 299 (3.86), 336 (3.80), 351 (3.72), 367 (3.48) nm; ^{1}H and ^{13}C NMR data (DMSO-d_6), see Table 2; (+)-LRESIMS *m/z* 305 $[M + H]^+$; (+)-HRESIMS *m/z* 327.0740 $[M + Na]^+$ (calcd for $C_{18}H_{12}N_2O_3Na$, 327.0740).
26. Soni, R.; Muller, L.; Furet, P.; Schoepfer, J.; Stephan, C.; Zumstein-Mecker, S.; Fretz, H.; Chaudhuri, B. *Biochem. Biophys. Res. Commun.* **2000**, *275*, 877.
27. Kuzmich, A. S.; Fedorov, S. N.; Shastina, V. V.; Shubina, L. K.; Radchenko, O. S.; Balaneva, N. N.; Zhidkov, M. E.; Park, J. I.; Kwak, J. Y.; Stonik, V. A. *Bioorg. Med. Chem.* **2010**, *18*, 3834.
28. Baron, P. S.; Neve, J. E.; Camp, D.; Suraweera, L.; Lam, A.; Lai, J.; Jovanoic, L.; Nelson, C.; Davis, R. A. *Magn. Reson. Chem.* **2013**, *51*, 358.